

Toughening behaviour of rubber-modified thermoplastic polymers involving very small rubber particles: 2. Rubber cavitation behaviour in poly(vinyl chloride)/methyl methacrylate-butadiene-styrene graft copolymer blends

D. Dompas and G. Groeninckx*

Catholic University of Leuven, Laboratory of Macromolecular Structural Chemistry, Celestijnenlaan 200F, B-3001 Heverlee, Belgium

and M. Isogawa and T. Hasegawa

Kaneka Corporation, Plastics Research Laboratories, 1-8 Miyamae-Machi, Takasago-cho, Takasago-shi, Hyogo 676, Japan

and M. Kadokura

*Kaneka Belgium NV, Head-Office Plant, Nijverheidsstraat 16, 2260 Westerlo-Oevel, Belgium
(Received 26 January 1994)*

Real-time stress-whitening experiments were performed on initially transparent poly(vinyl chloride) (PVC)/methyl methacrylate-butadiene-styrene graft copolymer (MBS) blends containing very small MBS rubber particles. The chemical composition of the different MBS rubber particles was held constant and it was found that the onset of internal rubber cavitation in the blends during a tensile test depends only on the size of the rubber particles. The real-time, stress-whitening experiments indicate that the resistance against cavitation increases with decreasing rubber particle size. Small particles are unable to cavitate. This is further confirmed independently on the basis of transmission electron microscopy observations and density measurements on the deformed samples.

(Keywords: rubber toughening; particle size; PVC/MBS blends)

INTRODUCTION

Substantial enhancement of the toughness of brittle or notch-sensitive polymers can be achieved by dispersing rubber particles in the polymer matrix. In pseudoductile thermoplastic matrices which deform preferentially by shear yielding, the major toughening mechanisms are thought to be cavitation of the rubber particles and shear yielding of the matrix¹⁻³. Rubber cavitation occurs first if the Poisson ratio of the rubber is close to 0.5^{4,5}. This relieves the hydrostatic tension in the material and thereby promotes ductile matrix shear yielding.

According to the interparticle distance concept^{1,6}, the toughness improves with improved dispersion, i.e. with decreasing rubber particle size. However, experiments have shown that if the rubber particle size is decreased below a critical value of ~200 nm, the impact toughness of the blend substantially decreases and approaches the value of the unmodified matrix⁷⁻¹⁰. There appears to be a critical particle size below which the toughening

efficiency of the rubber is practically zero. As a possible explanation, it has been suggested that small particles are not able to cavitate^{7-9,11,12} and therefore do not relieve the hydrostatic tension in the material to promote ductile shear yielding.

Therefore, because of the importance of rubber cavitation in impact mechanical behaviour and the suggestion that small particles are unable to cavitate, the relationship between cavitation strain and rubber particle size is evaluated in this paper. In general, cavitation can be studied by tensile dilatometry^{1,3} or by light^{3,4,9} and X-ray¹⁴ scattering techniques. The sensitivity of the scattering methods is higher than that of tensile dilatometry. Scattering techniques, however, can only readily be applied if the rubber-modified systems are sufficiently transparent for the selected wavelength. This is not the case for most rubber-toughened materials; the contribution from the light scattering by the second-phase particles in general dominates over the light scattered as a result of the internal cavitation during the deformation. For this reason, it has been decided to perform our

* To whom correspondence should be addressed

cavitation study on blends of poly(vinyl chloride) (PVC) with methyl methacrylate-butadiene-styrene graft copolymers (MBS). Transparent blends of these two components can be produced by matching the refractive index of the MBS rubber to that of the PVC matrix^{15,16}. The blend obtained is highly transparent and thus forms an ideal material for study of the cavitation by light scattering.

The results of this investigation confirm that the resistance of rubber particles against cavitation increases with decreasing particle size and that there exists a critical particle size for cavitation. Particles with a size below 150 nm are unable to cavitate. In the following paper¹⁷, the concept of the critical particle size for cavitation will be used to explain the impact toughness of these PVC/MBS blends.

EXPERIMENTAL

Materials

MBS rubber particles are particularly well designed for blending with PVC; PVC/MBS blends combine a high transparency with an improved impact strength. The MBS rubber particles are core-shell impact modifiers and consist of an elastomeric core of a random styrene-co-butadiene copolymer (SBR) and a glassy shell composed of a copolymer of styrene (St) and methyl methacrylate (MMA), which is grafted on to the SBR. The MMA component in the shell is miscible with PVC¹⁸. This enhances the dispersion of the MBS rubber particles in the PVC matrix.

The chemical composition (monomer ratio) of the core and the shell are dictated by the requirement for refractive index matching with the matrix. For this reason, the SBR rubber core in this study consists of a butadiene (Bd)/St weight ratio of 77/23; this is synthesized by radical emulsion copolymerization. To this monomer mixture, a small amount (a few percent) of crosslinking agent is added so that the crosslink density of the SBR equals 4.3×10^{25} crosslinks per cubic metre. The St-MMA shell is grafted on to the SBR core by a radical graft emulsion copolymerization, and has a MMA/St weight ratio of 50/50. The core/shell weight ratio is either 60/40 or 70/30.

The MBS particle size is controlled by agglomeration (AGGL), aggregation (AGGR) or 'grow-out' (GO) of the particles¹⁶. The GO procedure involves an emulsion polymerization in which the particle size is controlled by the number of SBR particles that are initiated, followed by the grow-out of the particles to the desired size by further polymerization. The terms agglomeration and aggregation are used to describe a procedure where the rubber particles are destabilized in the emulsion during polymerization in a controlled manner, so that a limited number of latex rubber particles coalesce together to form larger particles. AGGR is used to describe a destabilization in which the small spherical particles retain their identity in the larger aggregates. On the other hand, AGGL implies the conversion of a number of small particles into a single larger spherical particle.

The grafting procedures can also be altered. The St-MMA shell can be synthesized in one stage as a random copolymer of St and MMA grafted on to the SBR core. Alternatively, the shell can be synthesized in two stages^{19,20}; first, PMMA is grafted on to the SBR core, and then PS, or vice versa. Clearly, the molecular microstructure of the grafted chains will be different but

the overall MMA/St weight ratio remains constant at 50/50 to ensure transparency in the blends with PVC. In the two-stage process, the covering layer of the PMMA homopolymer is highly compatible with the PVC. This will influence the adhesion between MBS and PVC, but this aspect, however, will not be treated in this present study.

The size of the MBS particles on the emulsion latexes was characterized by dynamic light scattering (d.l.s.) using a Nicomp apparatus. Independently, particle sizes were characterized by the light transmission intensity of the latex and by transmission electron microscopy on the PVC/MBS blends. Essentially, the same average particle size was obtained by the three methods. The different particle types and their average sizes are summarized in Table 1.

Blend preparation

Powder blends of PVC compound with 10 phr MBS were prepared at room temperature. The PVC compound was composed of 100 phr PVC (*K* value = 57), 2 phr octyltin mercaptide (heat stabilizer), 0.8 phr glycerine ricinolate and 0.2 phr ester of montanic acid (lubricant). The mixtures were processed by roll milling at 170°C for 5 min. The films from the roll mill were then pressed into sheets by compression moulding at 190°C for 15 min; the sheet thickness was 2 mm.

Transmission electron microscopy

Samples of the PVC/MBS blends were cut in to a size and a shape which were suitable for mounting on the specimen holder of an ultramicrotome. A tip of the block was carefully trimmed to form a sharp pyramid, with a cutting area of $\sim 0.01 \text{ mm}^2$. A Reichert-Jung Ultracut E machine, equipped with a glass knife, was used for this operation. The trimmed sample was then stained for 3 days in a 2 wt% aqueous solution of OsO₄. The dark stained block was again mounted in the holder and the ultrathin sectioning was started, using a diamond knife with a 35° facet angle. Sections were collected from the top part of the block in which the fixing effect was pro-

Table 1 Characteristics of the MBS particles employed in this study

Particle ^a	Polymerization technology	Core/shell ratio	SBR core diameter (nm)
M1	AGGR	60/40	130
M2	AGGR	60/40	165
M3	AGGR	60/40	205
M4	AGGR	60/40	255
M5	AGGL	60/40	260
M6	AGGL	60/40	300
M7	GO	60/40	92
M8	GO	60/40	178
M9	GO	60/40	195
M10	GO	60/40	255
M11	AGGR	70/30	120
M12	AGGR	70/30	150
M13	AGGR	70/30	195
M14	GO	70/30	77
M15	GO	70/30	113
M16	GO	70/30	150

^a Particles M11-M16 obtained by a two-stage graft copolymerization

duced. The section thickness was set at 70 nm, using a cutting speed of $1.5\text{--}3\text{ mm min}^{-1}$. These ultrathin sections were then ready for electron microscopy examination.

Transmission electron microscopy (TEM) investigations were performed on a Philips CM-10 transmission electron microscope, operating at 60 kV.

Morphology

The TEM study was performed on both undeformed and deformed blends. For the undeformed blends, at least five micrographs (magnification $\times 19\,000$ on screen) were taken in order to obtain statistically relevant data for the average rubber particle size in the blend. The magnification was further calibrated with two polystyrene (PS) latexes of known particle sizes, i.e. 109 and 312 nm in diameter. Since OsO_4 only stains the double bonds of the butadiene, the particle sizes that are obtained by this method represent the sizes of the SBR rubber cores. These values are given in Table 1.

Deformation mechanisms

For the PVC/MBS blends (deformed in uniaxial tension), ultrathin sections from the necked part of the samples were cut in such a way that the investigated area was parallel to the deformation direction. This allows us to visualize crazes, elongated particles and rubber cavitation, if these features are present.

Tensile tests

Uniaxial stress-strain experiments were performed with an Instron Series 1121 tensile testing instrument at room temperature (20°C), using an operating speed of 10 mm min^{-1} . Dumb-bell shaped test specimens, with a cross-section of $10 \times 2\text{ mm}^2$ and a gauge length of 20 mm were used.

Real-time stress-whitening experiments

The phenomenon of stress-induced whitening in rubber-modified polymers^{21,22} is well known, and has been attributed to voiding in the sample. For example, when rubber particles cavitate the light will be scattered due to the large difference in refractive index between the void and the matrix. However, most toughened plastics are not suitable for the study of cavitation by light scattering techniques because the light scattered from the second-phase rubber particles themselves already produces a high optical opacity that cannot be distinguished from stress-whitening. Therefore, transparent blends of PVC with MBS, in which the refractive indices of both phases are matched, were used in this study. This gave ideal materials for the study of cavitation by optical techniques.

In this present study, the initiation of stress-whitening during a tensile stress-strain experiment was determined, because this represents a measure of the ease of cavitation of the different modifiers. For the examination of stress-whitening in real-time, a camera was mounted on the Instron draw-bench. The experimental set-up is shown schematically in Figure 1.

Light from a stabilized white light source is focused on a dumb-bell shaped test specimen during a tensile stress-strain experiment. The light source produces a constant light intensity with a standard variation for the latter of $\sim 0.3\%$. The angle of incidence is 30° , with respect to the normal on the sample surface. A charged coupled device (CCD) camera is positioned along the

normal on the sample surface, and images are sent from the camera to a personal computer. Each image is composed of 512×512 points, with each point having a value between 0 and 255. This value is a relative measure of the light intensity (stress-whitening) on that point in the image.

The undeformed PVC/MBS sample is highly transparent, with the front and the back side of the sample being parallel and very flat, and containing only a minimum of surface defects. Under these conditions, most of the light will pass undisturbed through the sample. However, as soon as cavities initiate in the sample, the light intensity at the camera position increases dramatically, due to the light scattered by the cavitated particles. Therefore, the detection of cavitation by this method is very sensitive. The sensitivity of this method in terms of the scattering power of the spherical particles, as calculated from the Mie theory, is discussed in the Appendix.

Some caution must be taken regarding interpretation of the light scattering data. As well as light scattering from voids in the material, light scattering can, in principal, also result from a change in the refractive index of the two phases. The refractive indices, both parallel and perpendicular to the deformation, will change due to the molecular orientation of the material during the tensile experiment (birefringence). It can be expected that the refractive index variation is small in the elastic part of the test. Nevertheless, in order to confirm this statement, PVC/MBS blends were prepared with different degrees of orientation by compression moulding in the

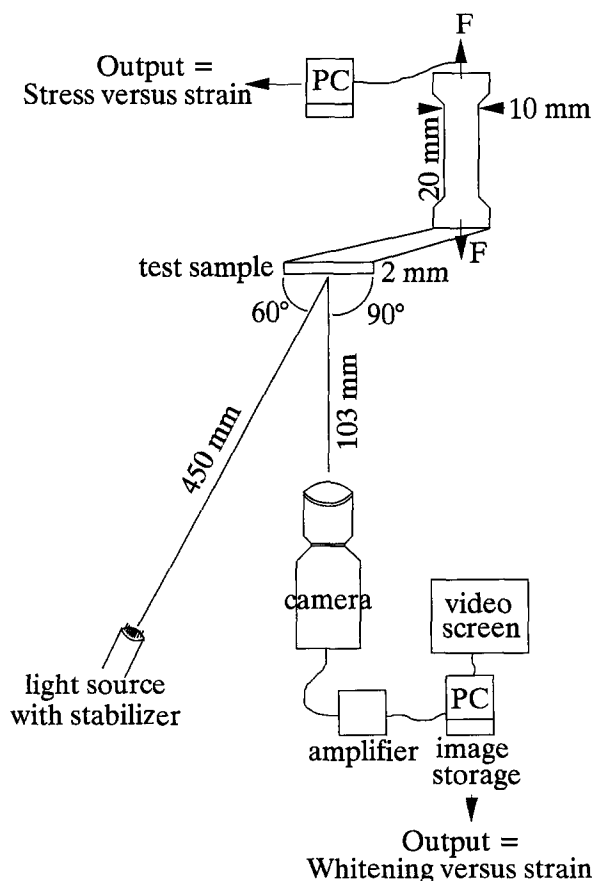


Figure 1 Schematic representation of the experimental set-up for the determination of stress-whitening during a tensile stress-strain experiment

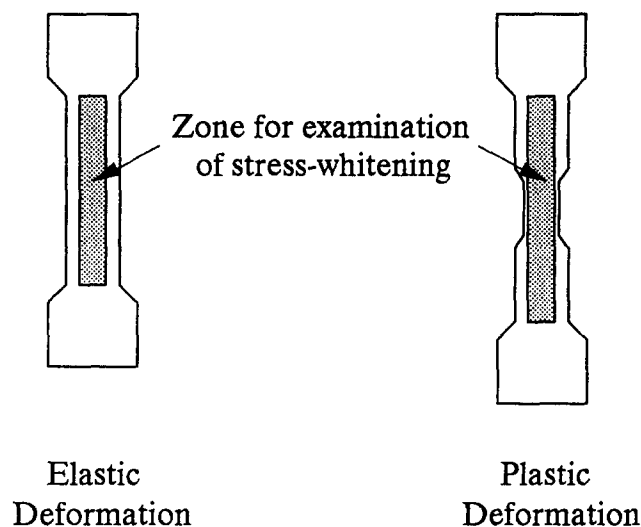


Figure 2 Schematic representation of the parts of the specimen that are taken for stress-whitening analysis, shown for two different deformations

melt, where cavitation cannot occur. The degree of orientation was then derived from measurements of the natural draw ratio. This compression moulding procedure gave a 10% variation in draw ratio. A 10% variation in molecular orientation is comparable to the yield strain in the PVC/MBS blends. In this range of molecular orientation, the optical opacity of the PVC/MBS blend material was not affected. It is therefore believed that the light scattering in the elastic region of the deformation experiment must arise from cavities generated in the blend, and not from a change in refractive index as a result of orientation. In addition, molecular orientation is also present in various application products of these PVC/MBS blends, such as, e.g. PVC/MBS bottles. If orientation were to strongly affect the optical properties of the end product, then achieving transparency in these materials would be a nearly impossible task. It thus seems justified to state that the observed light scattering in our systems in the elastic part of the test does not originate from birefringence effects, but from voiding in the material.

In order to maximize the acquisition speed for collecting data, only the central region of the deforming sample was taken for further analysis. This situation is indicated in Figure 2 for two different deformations, one in the elastic part of the test and one in the plastic part. The initial situation corresponds to an image of 221×70 points, or $\sim 20 \times 6$ mm. The length of the image varies, as indicated in the figure, together with the deformation at a speed of 10 mm min^{-1} . In this way, the area for investigation of the scattered light intensity is always the central part of the specimen between the sample enlargements.

Relevant information from the two-dimensional images is obtained using a program written in Turbopascal. This program evaluates the average stress-whitening intensity and the percentage whitening of the total investigated area as a function of strain. The cavitation strain is then derived from the percentage whitening *versus* strain curve. These different aspects can be briefly defined as follows:

Definition 1.

The *average stress-whitening intensity* is defined as the average of all light intensity values on every point of

the investigated image. It is a relative measure of the stress-whitening (light scattering) intensity, and has a value between 0 and 255.

Definition 2.

The experimental set-up using a camera has the advantage of evaluating the stress-whitening intensity independently on every point with dimensions of 0.1×0.1 mm in the deforming sample. If shear yielding starts prior to rubber cavitation, then stress-whitening would be restricted to the shear bands. If the reverse is true, then stress-whitening is not localized but is spread over the whole specimen. The *percentage whitening of the total investigated area* therefore gives an insight into the evolution of cavitation in the whole sample.

Definition 3.

The *cavitation strain* is defined as the strain corresponding to whitening in 50% of the total investigated area (see definition 2). This definition is chosen because the percentage whitening *versus* strain curve has a very steep slope at this point (see later). Consequently, the experimental standard variation at this point is very low and the *cavitation strain* is accurately defined.

Density measurements

The densities of the undeformed PVC/MBS samples and of the necked regions of the samples deformed in a uniaxial tensile test were measured at 25°C using Archimedes' principle (ASTM D-792). The method corrects for both the buoyancy of air and also for soaking of the hook in the immersion fluid.

The immersion liquid that was used was a low-viscosity silicon oil (2 cSt), with a density of $0.87295 \text{ g cm}^{-3}$ at 25°C . A hole of 1 mm diameter was drilled in the samples, and these were then immersed in the silicon oil by means of a small hook. The absolute values of the densities obtained by this method are in very good agreement with those reported in the literature, and have a standard deviation which is better than 0.0004 g cm^{-3} .

RESULTS AND DISCUSSION

Real-time stress-whitening data

Figure 3 illustrates the average stress-whitening intensity (definition 1), the percentage whitening (definition 2) and the tensile stress, all as a function of the strain, up to a longitudinal strain of 20% for PVC/MBS blends with large and small MBS particles.

In the initial stage of the deformation, the specimen remains transparent and the average stress-whitening intensity is practically zero, and remains constant. At a strain of the order of 4 to 8% (in the elastic part of the stress-strain curve), and depending on the particle size of the modifier, the average stress-whitening intensity, as well as the percentage whitening, both suddenly start to increase. This arises from cavities being generated in the blend under the applied elastic deformation.

The *average stress-whitening intensity* (dashed lines) increases substantially further after the yield point ($\epsilon_y = 8\%$). Optical examination of the samples revealed that the stress-whitening was much higher in the shear bands than in the rest of the test specimen, while the rest of the sample essentially remained at the same whitening level, or even decreased slightly, together with the stress. Three explanations can be given for the enhanced stress-whitening in the shear bands: (i) the cavities

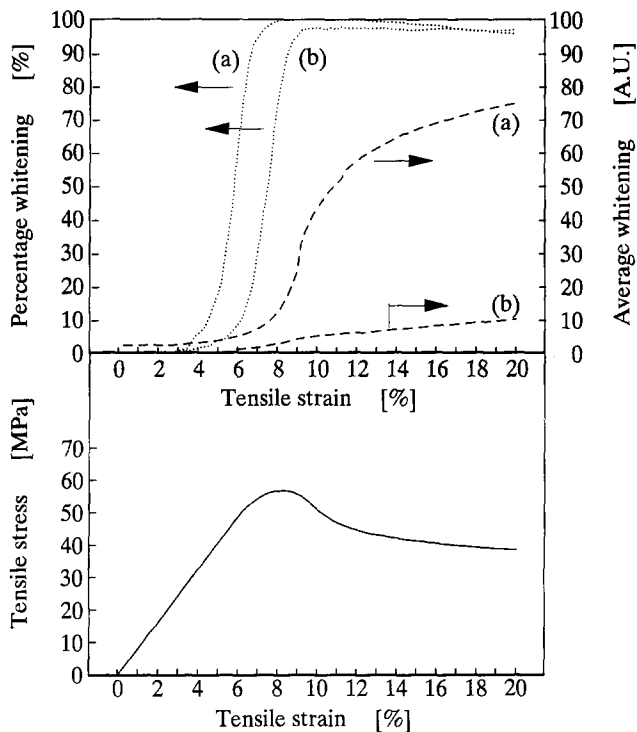


Figure 3 Examples of the type of information that can be obtained from analysis of stress-whitening in PVC/MBS blends by using the experimental set-up shown in Figure 1, namely the average stress-whitening intensity, the percentage whitening and the tensile stress, all as a function of the tensile strain: (a) large particles; (b) small particles

generated in the elastic region will expand further due to the large plastic strains in the shear bands, (ii) shear yielding further promotes cavitation, so that a larger number of cavities are generated, or (iii) the birefringence effect cannot be neglected during plastic deformation due to the pronounced molecular orientation in the shear bands. With the present technique, however, it is not possible to make a distinction between these three mechanisms.

The *percentage whitening* (dotted lines) is zero in the initial stage of the deformation, because the sample is transparent and therefore no light is scattered. At a strain of the order of 4 to 8%, the percentage whitening starts to rise as the whitening is spread out homogeneously over the whole sample area. Complete whitening over the whole sample area (i.e. 100%) is usually realized prior or close to the yield point. This suggests that cavitation occurs prior to shear yielding.

The stress-strain curve shown in Figure 3 is representative of all of the stress-strain curves of the PVC/MBS blends considered in this study. In other words, the Young's modulus, yield stress and yield strain are the same within experimental error for the different modifiers that are used. If the rubber particles are assumed not to bear stresses, then the yield stress is a function of the effective load-bearing area. This area is only a function of the effective rubber volume fraction in the blend and this is constant in the blends considered here. Therefore, for clarity, the stress-strain curves are omitted in the following figures.

Particle size effect

Comparing curves (a) and (b) in Figure 3, it can be observed that the average stress-whitening intensity increases more rapidly with increasing strain for blends

with a large rubber particle size (curve (a)). This can be explained from the relationship between the light scattering intensity and the rubber cavity size (see Appendix). The percentage whitening is also strongly influenced by the MBS particle size. Cavitation in the case of curve (a) for a large particle size occurs earlier than in the case of curve (b) for a smaller particle size. This clearly indicates that the resistance against cavitation increases with decreasing particle size.

A more detailed comparison of the percentage whitening as a function of strain for PVC/MBS blends with different SBR particle sizes is given in Figure 4. Since the blends remain transparent in the initial stage of the deformation, the percentage stress-whitening is then zero. Suddenly, but still in the elastic region of the deformation, the percentage whitening starts to rise and the whitening spreads through the sample. At least 50% of the total sample exhibits whitening in the elastic stage of the deformation. This behaviour is to be expected if rubber cavitation does indeed occur prior to plastic deformation of the matrix; if, in the opposite fashion cavitation is induced from matrix shear yielding, then stress-whitening would be concentrated in shear bands and the percentage stress-whitening *versus* strain curve should show a more gradual increase, starting in the plastic stage of the deformation. In this case, the percentage whitening would then be linearly related to the propagation of shear bands. Moreover, the stress-whitening clearly initiates well before the yield point ($\epsilon_y = 8\%$), indicating that even in uniaxial tensile tests with a moderate degree of triaxiality on the particles, cavitation can occur prior to shear yielding. On the other hand, it is surprising to observe that the yield stress and yield strain are not affected by the initiation of cavitation in the elastic region. Apparently, initiation of the plastic deformation in the matrix (shear yielding) is not influenced by the cavitation strains in these blends. The mild test condition (tensile test at low strain rate) with low triaxiality does not require the relief of the hydrostatic tension in the blend by cavitation for the initiation of matrix shear yielding. On the other hand, for Izod impact experiments with a pronounced triaxiality at the notch tip, relief of the hydrostatic tension by rubber cavitation is essential for the initiation of matrix shear yielding, as will be shown in the following paper¹⁷.

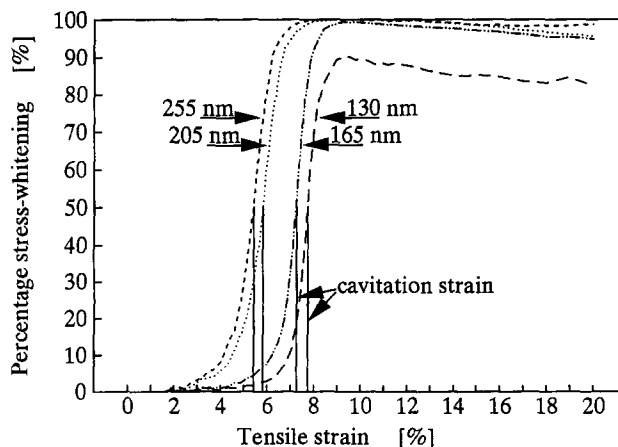


Figure 4 Comparison of the percentage whitening as a function of tensile strain for four different PVC/MBS blends (with MBS particles M1–M4 in Table I); rubber cavitation strains are indicated by the solid lines

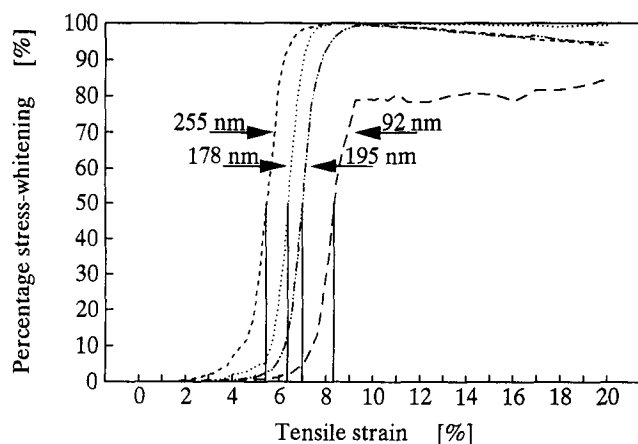


Figure 5 Comparison of the percentage whitening as a function of tensile strain for four different PVC/MBS blends (with MBS particles M7–M10 in Table I); rubber cavitation strains are indicated by the solid lines

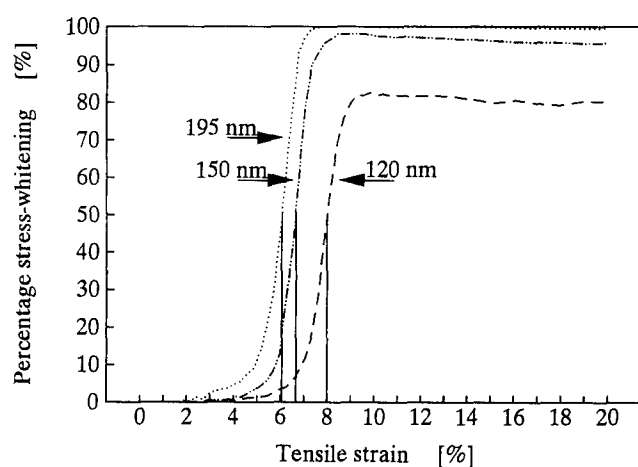


Figure 6 Comparison of the percentage whitening as a function of tensile strain for three different PVC/MBS blends (with MBS particles M11–M13 in Table I); rubber cavitation strains are indicated by the solid lines

Figure 4 demonstrates that the effect of particle size on the position of the sigmoidal curve is very pronounced. The larger the particle size, the earlier that cavitation occurs in the blend. This shows that large particles cavitate more readily than small particles. When the particle diameter is less than 150 nm, the cavitation strain approaches the yield strain. A size of 150 nm can thus be considered as a lower limit if cavitation is to occur in the elastic region of the tensile test prior to plastic deformation by matrix shear yielding. This critical particle size is also evidenced by the level of the percentage whitening that is reached. For the blends with a particle size larger than 150 nm, a level of 100% is reached either before or at the yield point. This means that the whitening is then spread out over the whole sample area. When the particles are smaller than 150 nm, the 100% level is not reached, again indicating that these smaller particles have a higher cavitation resistance. These phenomena are not just typical of MBS particles polymerized by the AGGR technology, but were also observed in the other PVC/MBS blends that were studied. Additional examples of various percentage whitening *versus* strain curves are given in Figures 5–7 for the blends of PVC with other types of

MBS. The particle size has exactly the same effect on the position and shape of the sigmoidal curve as for the blend discussed in Figure 4.

Interpretation of the stress-whitening data

In the previous paper of this series¹², it was demonstrated that rubber cavitation can be considered as a competition between the hydrostatic strain energy buildup in the particle and the surface energy required to create a new surface by cavitation. Rubber cavitation will then only occur if the total energy associated with the process decreases. The criterion for cavitation is given by the following¹²:

$$U_{\text{total}} = U_{\text{strain}} + U_{\text{surface}} \\ = -\pi/12K_r\Delta^2d_0^3 + (\gamma_r + \Gamma_{\text{sc}})\pi\Delta^{2/3}d_0^2 < 0 \quad (1)$$

where K_r is the rubber bulk modulus, γ_r is the van der Waals surface tension, Γ_{sc} is the chain scission energy per unit surface, d_0 is the rubber particle diameter and Δ is the relative volume strain of the particle. The first term is negative and corresponds to the hydrostatic strain energy in the particle that will be relieved by cavitation; this term is proportional to the third power of the particle size. The second term in the equation is positive and corresponds to the surface energy that is needed to create the new surface; this term is proportional to the second power of the particle size.

Cavitation can only occur if the volume strain of the particle reaches a critical level. Even in uniaxial tensile tests, the rubber particle experiences a volume strain because the Poisson ratio of the matrix is different from that of the rubber particle (0.5). The relative volume strain in the elastic region is given by the following relationship:

$$\Delta = (1 - 2\nu_m)\varepsilon \quad (2)$$

where ν_m represents the Poisson ratio of the (glassy) matrix and ε is the longitudinal strain. The relationship between the volume strain at which cavitation occurs and the particle diameter can be found by rearranging equation (1) as follows:

$$d_0 = \frac{12(\gamma_r + \Gamma_{\text{sc}})}{K_r\Delta^{4/3}} \quad (3)$$

This relationship¹² predicts that the cavitation strain (Δ

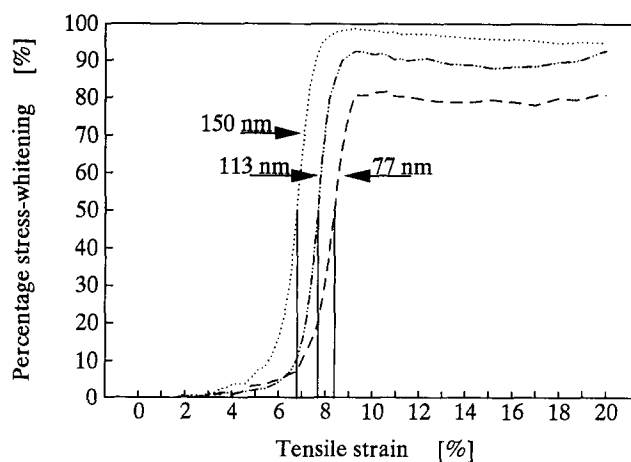


Figure 7 Comparison of the percentage whitening as a function of tensile strain for three different PVC/MBS blends (with MBS particles M14–M16 in Table I); rubber cavitation strains are indicated by the solid lines

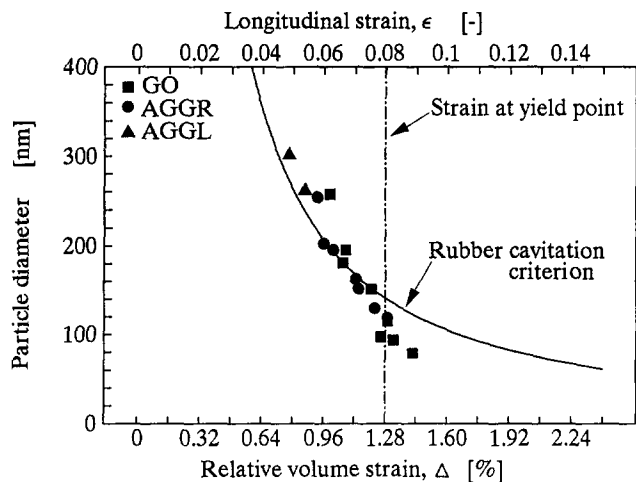


Figure 8 The relationship between the minimum particle diameter required for cavitation and the longitudinal (ϵ) and relative volume strain (Δ), where the relative volume strain is proportional to the longitudinal strain by $\Delta = (1 - 2\nu_m)\epsilon$. The experimental data (for three different types of MBS) are obtained from an analysis such as that given in Figures 4–7, and the theoretical line is obtained from equation (3) by using the following parameters: $K_r = 2$ GPa, $\gamma_r = 0.035$ J m $^{-2}$ and $\Gamma_{sc} = 0.035$ J m $^{-2}$

or ϵ) increases with decreasing particle diameter (d_0), in agreement with the observations given in Figures 4–7.

In order to compare equation (3) more quantitatively with the experimental cavitation strains the molecular and elastic parameters of equation (3) have to be specified. The bulk modulus K_r for SBR is ~ 2 GPa, while γ_r for most rubbery materials is ~ 0.035 J m $^{-2}$ (ref. 23). The Poisson ratio of PVC is 0.42 (ref. 23), with the chain scission energy per unit area (Γ_{sc}) being dependent on the crosslinking density of the rubber particle. A simplified calculation for a crosslinking density of 4.3×10^{25} crosslinks per cubic metre has given Γ_{sc} to be 0.035 J m $^{-2}$ (ref. 12).

Figure 8 compares the experimental (data points) and theoretical (equation (3), full line) relationship between the particle size and the cavitation strain for PVC/MBS blends. The experimental cavitation strain is the average of four experiments for every blend material; the experimental standard deviation for the cavitation strain is of the order of 0.4%.

This figure confirms that the cavitation resistance is governed by the rubber particle size; in a uniaxial tensile experiment, small particles cavitate at a higher strain than large particles. This trend is also expected from the model of internal cavitation (equation (3)); theory (full line) and experiment (data points) appear to be in good agreement on an absolute scale. An extensive and profound evaluation of the model, however, can only be performed in the case of a wider range of particle sizes. Unfortunately, neither larger nor smaller particles were available for these experiments. Nevertheless, it is clear that the resistance against cavitation increases with decreasing particle size. If it is assumed that cavitation must occur in the elastic deformation region, at a longitudinal strain below 8%, then the minimum particle size for cavitation is found to be 150 nm. This is in agreement with the analysis of the curves given in Figures 4–7 and demonstrates that very small particles cannot cavitate.

Transmission electron microscopy investigations

The fact that small particles are unable to cavitate can be demonstrated by transmission electron microscopy.

For this purpose, ultrathin sections were taken in the necked region of PVC/MBS test specimens that had been deformed in uniaxial tensile experiments. The sections were taken parallel to the deformation direction so that eventual crazes could also be detected. Prior to ultrathin sectioning, the specimens were stained and hardened with OsO $_4$.

On all of the transmission electron micrographs, regardless of the MBS type, small particles were found to deform only by elongation, while large particles were found to deform by elongation and voiding. A more profound analysis of the relationship between the MBS type and the microvoiding mechanism will be presented elsewhere²⁴. Representative micrographs are given in Figures 9 and 10 for a PVC/MBS blend with small and large particles, respectively. The MBS rubber in the blend deforms mainly by particle elongation in the case of small particles, and by rubber cavitation and particle elongation in the case of the larger particles. Crazes were not found in the micrographs. The transmission electron micrographs shown here confirm earlier observations¹⁵ on PVC/MBS blends that small particles do not cavitate. Furthermore, transmission electron micrographs of nylon-6/polybutadiene blends⁹ revealed that particles below 200 nm also do not cavitate in these blends. The inability of small particles to cavitate is the reason for the decrease in impact strength of the nylon-6 and PVC blends below a critical particle size^{7–9,12,17}.



Figure 9 Transmission electron micrograph of a PVC/MBS blend with a SBR particle size of 82 nm (MBS, AGGL type), deformed in uniaxial tension

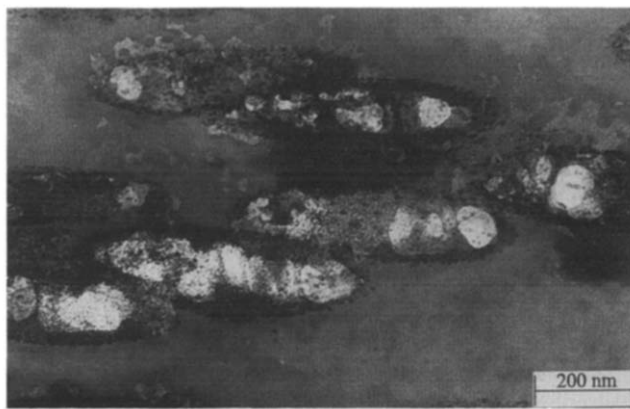


Figure 10 Transmission electron micrograph of a PVC/MBS blend with a SBR particle size of 255 nm (MBS, GO type), deformed in uniaxial tension

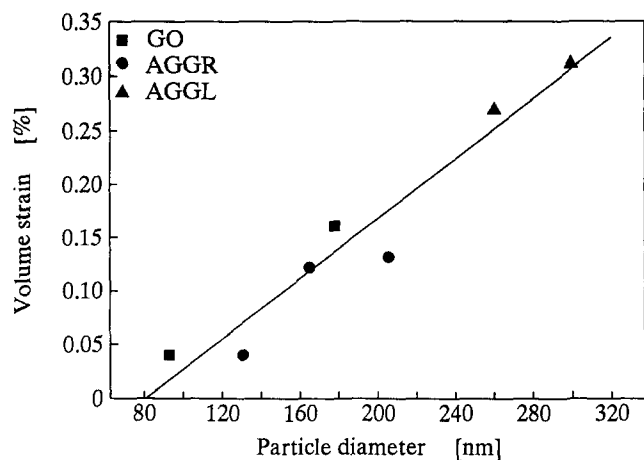


Figure 11 Volume strain in the necked region of dumb-bell shaped specimens of three different types of MBS, tested in uniaxial tension as a function of the rubber particle size in the blend

Volume strain measurements

Internal rubber cavitation, like any other voiding process, results in a decrease of the density of the material or an increase in volume. The relative volume strain ($\Delta V/V_0$) of the material is given by the following:

$$\Delta V/V_0 = f_p N_p V_c \quad (4)$$

where f_p is the fraction (by number) of cavitated particles, N_p is the number of rubber particles per unit volume and V_c is the cavity volume of one internally cavitated particle. The cavity volume is proportional to the rubber particle volume as follows:

$$V_c = K V_r \quad (5)$$

where K is a proportionality factor and V_r is the rubber particle volume. The number of particles per unit volume is inversely proportional to the rubber particle volume as follows:

$$N_p = \Phi_{\text{MBS}}/V_r \quad (6)$$

where Φ_{MBS} is the volume fraction of the MBS particles, which for this study was held constant at a value of 0.12. Accordingly, equation (4) can be rewritten in the following way:

$$\Delta V/V_0 = f_p \Phi_{\text{MBS}} K \quad (7)$$

If the tendency to cavitate is a function of the rubber particle size as shown before, then particle size and volume strain should also be related. However, if internal cavitation is a purely stochastic process, where the fraction of cavitated particles (f_p) is constant and independent of the particle size, then it is clear from equation (7) that the volume strain should be independent of the rubber particle size (d_0). Moreover, the fraction of internally cavitated rubber particles can be computed from equation (7) providing that K is known. This proportionality factor can be estimated from examination of the transmission electron micrographs. This was carried out by Breuer *et al.*¹⁵, who found that the volume of cavitated MBS rubber particles was 7–9% higher than the volume of the undeformed MBS rubber particles. Taking $K = 0.08$ and $\Phi_{\text{MBS}} = 0.12$, this gives the following:

$$\Delta V/V_0 \sim 0.01 f_p \quad (8)$$

Equation (8) provides a rough estimate of the fraction of cavitated particles from volume strain measurements.

Besides being material dependent, the volume strain is also dependent on the deformation history. The types of deformation before yielding, during necking and during neck propagation are different. In order to compare the different materials, only the neck-propagated part of the sample was considered. The volume strain was then determined from the density difference between the deformed and undeformed material. An average of 18 test specimens per material was taken, with the standard error in this experiment found to be 0.03%.

Figure 11 demonstrates the relationship between the volume strain and the MBS particle size for three different types of MBS. The volume strain in these materials is typically less than 0.5%. Although considerable stress-whitening was observed in these materials, this indicates that at least 99.5% of the deformation in the blend is due to shear yielding of the matrix. Since crazes were not observed in the transmission electron micrographs of these blends, the remaining 0.5% volume strain is entirely due to rubber cavitation. Based on the simplified analysis of equation (8), the fraction of cavitated MBS particles is estimated to lie between 0 and 50%, and from Figure 11 it is clear that this fraction is higher for blends with larger particle sizes. In other words, the fraction of internally cavitated particles and the volume strain of the blend increase with increasing rubber particle size: the tendency to cavitate and to relieve the weak triaxiality in a uniaxial tensile test is apparently more pronounced in blends with larger rubber particles. This confirms the relationship between the ease of cavitation and the particle size of the modifier.

CONCLUSIONS

The cavitation resistance of SBR rubber particles in PVC/MBS blends is dependent on the rubber particle size. Small particles require a higher volume strain for cavitation than large particles. The inability of small particles to cavitate has been found independently by real-time stress-whitening, transmission electron microscopy and the density decrease in uniaxial tensile stress-strain experiments. In the previous paper in this series¹², it was shown that cavitation can be considered as the result of a competition between the strain energy of the particle relieved by cavitation and the surface energy required to create the new surface. In the equation which describes the criterion for cavitation, the fact that the first term is proportional to the third power of the particle size, with the second term only to the second power of the particle size, explains why small particles are unable to cavitate. In addition, the theoretical critical particle size for cavitation is in complete agreement with the experimental value. In the following paper¹⁷, the concept of the critical particle size for cavitation will be applied in order to explain the impact mechanical behaviour of the PVC/MBS blends.

ACKNOWLEDGEMENTS

Two of the authors (G. Groeninckx and D. Dompas) are indebted to Kaneka Belgium NV and the Nationaal Fonds voor Wetenschappelijk Onderzoek for the financial support given to their laboratory. G. De Geests and B. Vanderschueren of the Laboratorium voor Menselijke Erfelijkheid, Catholic University of Leuven, are thanked for the availability of the transmission electron microscope

and for their help with interpreting the results obtained. Valuable discussions concerning the results presented in this paper were held with K. Isayama and R. Nishimura, and also with K. Dijkstra and J. W. Boode.

REFERENCES

- 1 Wu, S. *Polym. Int.* 1992, **29**, 229
- 2 Borggreve, R. J. M., Gaymans, R. J., Schuijjer, J. and Ingen Housz, J. F. *Polymer* 1987, **29**, 1489
- 3 Tse, A., Shin, E., Hiltner, A., Baer, E. and Laakso, R. *J. Mater. Sci.* 1991, **26**, 2823
- 4 Parker, D. S., Sue, H.-J., Huang, J. and Yee, A. F. *Polymer* 1990, **31**, 2267
- 5 Huang, Y. and Kinloch, A. J. *Polymer* 1992, **33**, 5338
- 6 Wu, S. *Polymer* 1985, **26**, 1855
- 7 Oostenbrink, A. J., Dijkstra, K., Wiegiersma, S., v.d. Wal, A. and Gaymans, R. J. PRI International Conference on Deformation, Yield and Fracture of Polymers, Cambridge, April, 1990
- 8 Oshinski, A. J., Keskkula, H. and Paul, D. R. *Polymer* 1992, **33**, 268
- 9 Dijkstra, K. *PhD Thesis*, University of Twente, The Netherlands, 1993
- 10 Wrotecki, C., Heim, P. and Gaillard, P. *Polym. Eng. Sci.* 1991, **31**, 213
- 11 Wu, S. *J. Appl. Polym. Sci.* 1988, **35**, 549
- 12 Dompas, D. and Groeninckx, G. *Polymer* 1994, **35**, 4743
- 13 Borggreve, R. J. M., Gaymans, R. J. and Eichenwald, H. M. *Polymer* 1989, **30**, 78
- 14 Bubeck, R. A., Buckley, D. J., Kramer, E. J. and Brown, H. R. *J. Mater. Sci.* 1991, **26**, 6249
- 15 Breuer, H., Haaf, F. and Stabenow, J. *J. Macromol. Sci.-Phys.* 1977, **14**, 387
- 16 Dunkelberger, D. L. and Dougherty, E. P. *J. Vinyl Technol.* 1990, **12**, 212
- 17 Dompas, D., Groeninckx, G., Isogawa, M., Hasegawa, T. and Kadokura, M. *Polymer* 1994, **35**, 4760
- 18 Schurer, J. W., De Boer, A. and Challa, G. *Polymer* 1975, **16**, 201
- 19 Haaf, F., Breuer, H., Echte, A., Schmitt, B. J. and Stabenow, J. *J. Sci. Ind. Res.* 1981, **40**, 659
- 20 Terlemezyan, L., Mihailov, M., Kamburova, L., Ivanova, B., Gantchev, B. and Ivanova, G. *Acta Polym.* 1989, **40**, 279
- 21 Bucknall, C. B. 'Toughened Plastics', Applied Science, London, 1977
- 22 Kinloch, A. J. and Young, R. J. 'Fracture Behaviour of Polymers', Applied Science, London, 1983
- 23 van Krevelen, D. W. 'Properties of Polymers', Elsevier, Amsterdam, 1976
- 24 Dompas, D., Groeninckx, G., Isogawa, M., Hasegawa, T. and Kadokura, M. *Polymer* submitted
- 25 Dompas, D., Groeninckx, G., Isogawa, M., Hasegawa, T. and Kadokura, M., unpublished results
- 26 Kerker, M. 'The Scattering of Light and other Electromagnetic Radiation', Academic Press, New York, 1969

APPENDIX

Detection of rubber cavities by light scattering

In order to demonstrate the sensitivity of the real-time stress-whitening technique for the detection of internal rubber cavitation, (i) the light scattering of 'nearly' transparent PVC/MBS materials is measured, (ii) the scattering cross-sections of MBS particles and voids in a PVC matrix are compared with calculations based on the Mie theory, and (iii) the average size of internal rubber cavities is estimated, based on the assumption of an elastic relaxation of the rubber particle after internal rupture.

Step (i). The blends of PVC with MBS have been treated as perfectly transparent materials. In reality, the refractive index of the MBS particles is not perfectly matched to the refractive index of the PVC matrix. Measurements and theoretical estimations indicate that the refractive index of MBS in this study is 1.535,

compared to the refractive index of the PVC matrix which is 1.539²⁵. As a result of this refractive index difference, light is scattered by the MBS particles. The haze observed on 2 mm thick specimens of the blends is found to increase with increasing MBS particle size, but remains below 15%, even for the largest particles²⁵.

This phenomenon of light scattering by the dispersed rubber particles as a result of the imperfect matching of the refractive indices can be used to demonstrate the sensitivity of the real-time stress-whitening method. For this purpose, the average light scattering intensity of undeformed samples has also been measured using the experimental set-up shown in *Figure 1*; the results are given in *Figure A1*. This figure demonstrates that, in analogy with the quantitative haze measurements²⁵ and in accordance with light scattering theory, the average light scattering from the MBS particles increases with increasing particle size.

Step (ii). The above observations on nearly transparent materials is already an indication of the sensitivity of the method. However, in order to compare the light scattering from MBS particles with the light scattering from the same amount of voids in the sample, the Mie theory for light scattering has to be applied. According to this theory, the scattering cross-section (C_{sca}) for spherical particles is given by the following²⁶:

$$C_{sca} = \lambda_{eff}^2 / 2\pi \sum_{n=1}^{\infty} (2n+1)(|a_n|^2 + |b_n|^2) \quad (A1)$$

where λ_{eff} is the wavelength of the light in the material, and a_n and b_n are the Mie scattering coefficients, which are dependent on the particle size, the wavelength and the refractive indices of the matrix and the disperse phase.

Scattering cross-sections are calculated assuming a matrix with a refractive index of 1.539 (PVC), in which spherical particles, having a refractive index varying from 1.000 to 1.535, are dispersed. A refractive index of 1 corresponds to that of air and is therefore a measure of the scattering power from voids in the sample; a refractive index of 1.535 corresponds to that of MBS.

The results of the calculations of the scattering cross-sections of spherical particles are represented as a function of particle size in *Figure A2*. This figure indicates that both the particle size and the difference in refractive

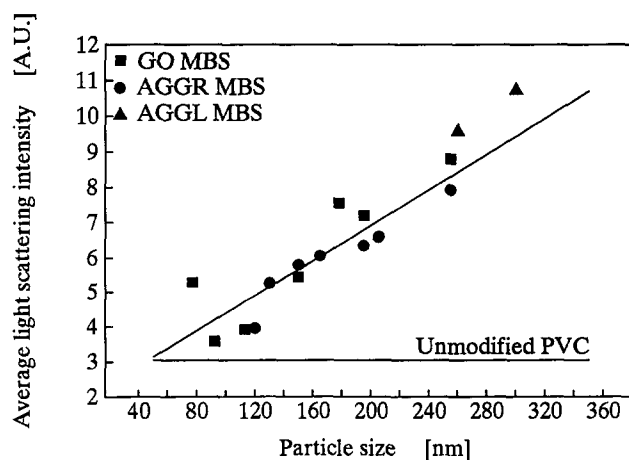


Figure A1 The relationship between the average light scattering in undeformed samples, measured using the experimental set-up shown in *Figure 1*, and the particle size of three different types of MBS

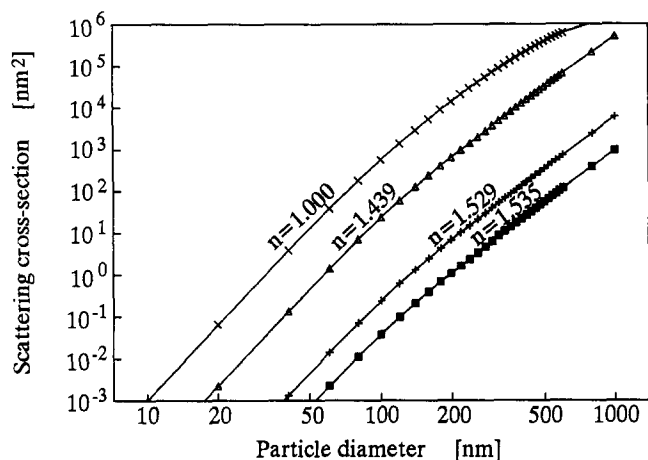


Figure A2 The scattering cross-section for spherical particles embedded in a matrix with a refractive index of 1.539 (PVC) as a function of particle size, for light with a wavelength of 500 nm. The refractive index (n) of the dispersed phase is indicated and ranges from 1 (air) to 1.535 (MBS); curves are calculated on the basis of the Mie theory

index between particle and matrix have a pronounced effect on the scattering cross-section of the particles. For example, below particle diameters of 100 nm, the scattering cross-section of a void ($n=1.000$) is more than 10^4 times higher than the scattering cross-section of a MBS particle ($n=1.535$) with the same diameter. Likewise, based on the Mie theory, the scattering cross-section of a MBS particle ($n=1.535$) of 200 nm is equal to the scattering cross-section of a void ($n=1.000$) of only 30 nm. It should be mentioned, however, that the light scattering intensity is also angular dependent. For particles with a size between 100 and 300 nm, such as the MBS particles, most

of the light is scattered in the forward direction. For particles with a size between 10 and 100 nm, the angular dependence is not so pronounced, and forward and backward scattered light have about the same intensity. The experimental set-up shown in *Figure 1* is thus particularly suitable for the detection of small particles such as rubber cavities.

Step (iii). The value of 30 nm should be compared with the void size of an internally cavitated rubber particle. This void size (d_i) can be estimated assuming a complete elastic relaxation of the elastomer after internal fracture and is dependent on the relative volume strain (Δ) of the material and the initial particle diameter (d_0) as follows:

$$d_i = \Delta^{1/3} d_0 \quad (\text{A2})$$

Taking Δ as 0.008, the cavity size from a rubber particle with an initial diameter (d_0) of 200 nm then becomes 40 nm. Since the scattering cross-section for very small particles is proportional to the sixth power of the particle size (Rayleigh scattering), the scattering cross-section of a void of 40 nm is much higher than the scattering cross-section of a void of 30 nm. Calculations estimate an increase in scattering cross-section by a factor of four. For nearly completely transparent materials, such an increase in scattering power has a very pronounced effect on the optical properties of the material²⁵.

On the basis of the above arguments, it is therefore concluded that the method of real-time light scattering presented here is sufficiently sensitive for the detection of light scattering by internal cavitation of the rubber particles, even when the void size is much smaller than the original rubber particle sizes.